MDPI

Article

Optimization of Conductive Fins to Minimize UO$_2$ Fuel Temperature and Radial Temperature Gradient

Kyle M. Paaren *, Pavel Medvedev and Robert Mariani

Idaho National Laboratory, 2525 Fremont Ave., Idaho Falls, ID 83415, USA
* Correspondence: kyle.paaren@inl.gov

Abstract: To further the development of low-enriched uranium fuels, precedence has been placed on delivering the same amount of power while lowering the fuel temperature and radial temperature gradient. To address this, modeling efforts have resulted in a novel design featuring conductive fins of varying thermal conductivities and geometries inserted into the fuel matrix. These conductive inserts were not allowed to exceed 6% of the original fuel volume. This constraint was imposed due to other designs displacing 10% of fuel volume. A parametric study was performed that consisted of 2.56 million BISON simulations involving varying fin characteristics (i.e., fin thermal conductivity, number, and geometry) to determine the optimal geometric configuration for a desired amount of fuel volume displaced. The results from this study show that the thickness and length of each fin affect the fuel temperature and temperature gradient more than varying the number and thermal conductivity of the fins. The parametric study resulted in the development of an optimized combination to produce the lowest peak fuel temperature, lowest radial temperature gradient, and highest temperature reduction for the amount of original fuel volume displaced. The simulations presented in this work will eventually be compared with irradiation experiments of similar fuel designs at Idaho National Laboratory's Advanced Test Reactor.

**Keywords:** BISON; simulation; finite element methods; fuel performance; UO$_2$

1. Introduction

Within a typical UO$_2$ pellet design for light-water reactors (LWRs), the limiting factor capping the power density of the fuel matrix is the high centerline fuel temperatures during operation. These temperatures are due to the ceramic UO$_2$ pellets' low thermal conductivity, which degrades with burnup. Despite the thermal conductivity of UO$_2$ limiting the power density, UO$_2$ continues to draw customers, as it is a dependable, proven fuel type with a high melting temperature, chemical stability for its oxide nature, and microstructural stability for its cubic type. These performance features and the large technology infrastructure surrounding them have led to efforts to increase the thermal conductivity of UO$_2$ fuel so that the power density of the fuel or burnup may be increased without raising operating temperatures, or in the case of this study, how much temperature reduction can be achieved with the same power density.

There are two main types of LWRs used in commercial power production, being pressurized water reactors (PWR) and boiling water reactors (BWR). Each of these reactor types uses UO$_2$ fuel and zircaloy cladding for their power production, although the size of the assemblies is different due to how they produce power. High temperature reactors (HTR) also use UO$_2$ fuel for power production but operate at much higher temperatures by using helium or molten salt coolants compared with water in LWRs and PWRs. In all of these systems, reducing peak fuel temperature retains fission gas, extends safety margins, and extends burnup. Each of these leads to better fuel performance for a single and multi-batch loading, leading to cost savings and reducing the amount of stored waste just by reducing the fuel temperature while maintaining the same power.

Efforts to increase the thermal conductivity of UO_2 fuel include doping the pellets with beryllium-oxide, molybdenum, silicon carbide, and diamond/carbon at varying percentages to reduce fuel centerline temperatures [1–5]. Other solutions to increasing thermal conductivity of UO_2 include doping with uranium nitride fuel upwards to 62.3 wt% and gadolinium oxide up to 10 wt% [6,7]. The addition of these materials to evenly dope the UO_2 pellets succeeded in lowering the centerline fuel temperature of the fuel pellets but did little to change the radial temperature gradient of the UO_2 pellet. Other researchers explored dispersion fuels, but such fuels sacrifice uranium volume to the dispersion matrix, thus tending to increase core volume. This is seen in AREVA's design using 10% volume doped UO_2 dispersion fuel with SiC powder with spark plasma sintering [5]. This 10% fuel volume cap was implemented due to fuel enrichment and reactivity requirements to produce the same amount of power while lowering the peak fuel temperature. Using the SiC power in the fuel pellets was found to increase the thermal conductivity by up to 40%, a 250 K decrease in fuel centerline temperature, and a 100 K decrease in average fuel temperature when simulated in FRAPCON [5]. This pellet was designed and successfully irradiated in the Advanced Test Reactor (ATR) at Idaho National Laboratory (INL), although high thermal gradients caused chips and cracks during sintering. These gradients were present in ATR as well, as the thermal gradients may cause debonding and delamination between conductive inserts and the fuel matrix used in this work.

In addition to advancing the performance of UO_2 fuel itself, there have been advancements in Accident Tolerant Claddings (ATC) under the Accident Tolerant Fuels (ATF) program. Such claddings include 310 stainless steel, SiC, and FeCrAl and are in development to be tested against Zircoloy-4. The purpose of ATCs is to be more neutron resistant, offer neutronic improvements, and provide a higher yield strength compared with Zircoloy-4 [8,9]. This allows for better neutron economy and a better handling of pellet cladding mechanical interaction as fuel continues to swell as burnup increases. The increased yield strength also provides a larger elastic and plastic range during steady-state operations and accident conditions, such as blowdowns. The combination of advanced fuel technologies to reduce fuel temperature in conjunction with ATCs would further aid fuel performance and extend burnup past the current 62 GWD/MTHM limit [10].

Previous work conducted at Idaho National Laboratory's advanced low-enriched uranium fuel project focused on inserting disks and fins within a UO_2 fuel pellet to decrease the peak fuel temperature; this succeeded in reducing the peak fuel temperature and radial temperature gradient significantly, with linear heat generation rates (LHGR) of up to 50 kW·m^{-1} [11,12]. An example of this is shown in Figure 1. Prior work documented a six-fin design, and the corresponding results prompted the parametric analysis presented in this work, which was a rapid, "what-if" analysis of the design features over a range of conditions [11]. This six-fin design utilized evenly spaced fins within the UO_2 matrix and was also compared with a conductive disk design, with geometry similar to Figure 1 [13,14]. Conductive fins within this prior work were found to reduce peak fuel temperature more than conductive disks with the same amount of fuel volume displaced, with the temperature reduction being 867 K using molybdenum inserts [13–15]. This temperature reduction was able to bring the peak fuel temperature below the Halden threshold to limit fission gas release (FGR) [10]. The prior results for the six-fin design were used as a baseline for comparing peak fuel temperatures in this parametric analysis. The six-fin conductive insert design utilized molybdenum (thermal conductivity of 128 W·m^{-1}·K^{-1}) as the insert and did not account for a helium gap between the fuel and the cladding [13,14].
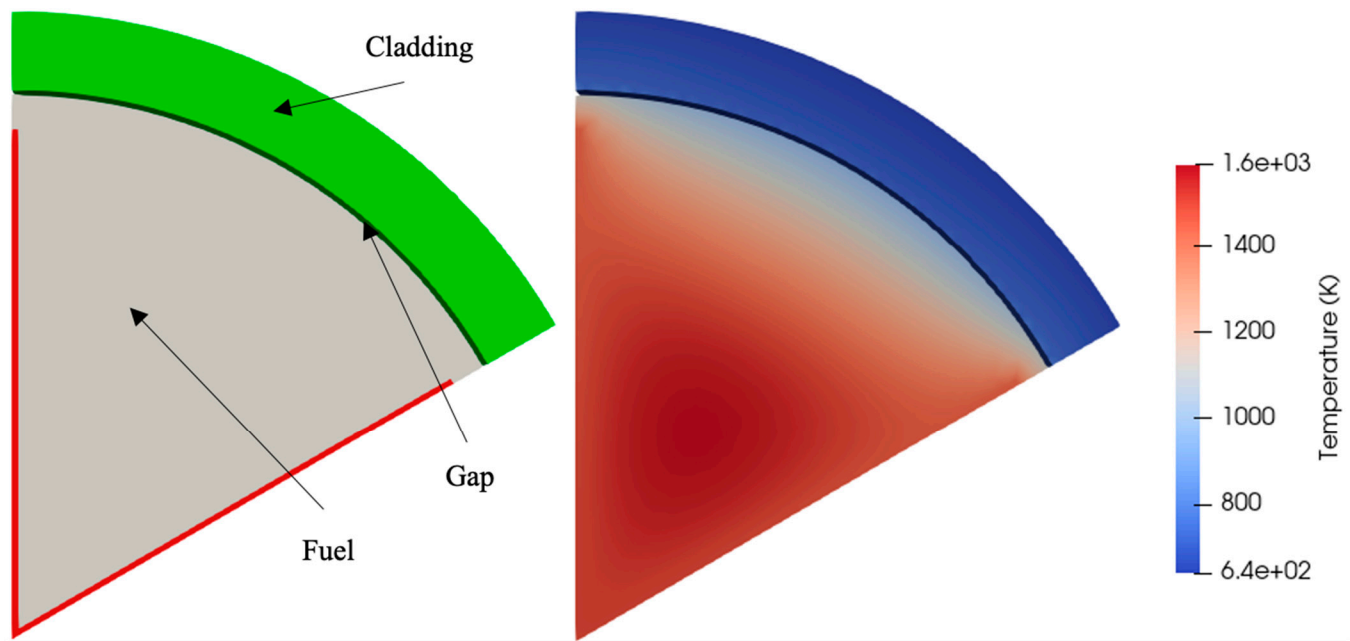
Figure 1. Standard UO$_2$ pellet wedge with a typical 6-fin design (**left**) and temperature distribution (**right**).

This work included a parametric analysis which varied the number of geometric configurations and fin thermal conductivity to account for different fin volumes while maximizing the decrease in peak fuel temperature past 250 K. Different materials used for conductive inserts in this analysis included various steels, molybdenum, beryllia, and synthetic diamond [1,2,4,16–18]. The benefit of this temperature reduction is that it allows for higher temperature safety margins during normal operation conditions and a greater threshold during accident scenarios. The work presented in this manuscript describes the thermal modeling results obtained within the BISON framework and offers the optimal thermal results from the parametric study using conductive fins with a fixed volume and a fixed LHGR of 50 kW·m^{-1}. BISON is a finite element-based nuclear fuel performance code applicable to a variety of fuel forms, including light water reactor fuel rods, TRISO particle fuel, and metallic rod and plate fuel. It is a multiphysics fuel analysis tool that solves fully coupled thermomechanical problems [19].

Conductive insert volumes up to 6% of the fuel volume were considered in this analysis, with the optimal conductive insert geometries for different fixed volumes presented. Depending on the amount of fuel volume displaced by the conductive fins and the thermal conductivity of the fins, a peak temperature reduction of ~1200 K may be achieved. Delamination of conductive fins from the UO$_2$ matrix was considered, with a delamination gap of 100 μm causing a ~200 K increase for molybdenum inserts. It is evident that higher thermal conductivity, more fins, and increased fin length and thickness produces lower peak fuel temperatures, but geometric configurations minimizing peak fuel temperature for specific fin volumes are not so obvious. Maximizing peak fuel temperature and gradient reduction for specific fuel volumes were explored in this work. Although this work only provides the thermal solution for conductive inserts in UO$_2$ fuel, the implications of this simplification and steps to model thermomechanical properties are discussed.

2. Methods

All BISON simulations conducted in this parametric study were based on a generic input file developed for only predicting the thermal performance of conductive inserts featuring varying geometries and material properties. In total, four parameters were varied to determine the optimal geometry for a desired amount of fuel volume displaced: the thermal conductivity of the insert, the number of fins inserted, the length of each fin, and the thickness of each fin. To assess the effects of these parameters on the peak fuel

temperature and radial temperature gradient, the LHGR of the simulation was fixed at 50 kW·m^{-1}. This was to ensure that the same amount of power was produced within each simulation regardless of the amount of fuel volume displaced by the conductive inserts. Since the volume of the fuel was adjusted to compensate for the inserted fin geometry, the total power of the UO$_2$ pellet had to be adjusted to keep the LHGR at 50 kW·m^{-1}. While this LHGR is higher than typical applications, its use increases the effects seen from varying the conductive insert parameters. The cladding thickness, pellet–cladding gap, pellet height, and pellet outer diameter were kept constant throughout the simulations.

In total, 2.56 million simulations were conducted in this parametric study to create a dataset for different conductive insert geometries. The thermal conductivities of the conductive fins were varied between 0.5 and 1024 W·m^{-1}·K^{-1} to simulate the different materials that might be used, such as glass, various metals, and diamond. The different materials considered are listed in Table 1. It is important to note that each of the thermal conductivities used in the BISON simulations was fixed and was not temperature dependent. It is recognized that cross-sections associated with material choices were not considered in this analysis and are planned for future work. The number of fins varied between 3 and 12, each with a length of 1.735–3.7125 mm, and the pellet radius was 3.96 mm. The fin thickness varied between 59.4 and 594 µm for each possible fin number, length, and material thermal conductivity. The dimensions for the fuel, cladding, and insert geometry and thermal conductivity variations simulated are listed in Table 2. Each BISON simulation included one UO$_2$ fuel pellet using the conductive fins as lines of symmetry in order to reduce computational time. The thermal conductivity of the conductive inserts was varied to represent a variety of different materials proposed to reduce the peak fuel temperature for a set volume.

Table 1. Thermal Conductivity of various materials.

Thermal Conductivity (W·m^{-1}·K^{-1})	Material
16–64	Various steels [16,17]
128	Molybdenum [2]
256	Beryllia [1]
512	Diamond (impure) [4]
1024	Synthetic diamond [18]

Table 2. UO$_2$ pin geometries.

Parameter	Solid UO$_2$ Pellet	Conductive Insert UO$_2$ Pellet
Pellet OD (mm)	7.92	7.92
Cladding OD (mm)	9.14	9.14
Cladding ID (mm)	8.00	8.00
Fuel Pin Height (cm)	1	1
Insert Thermal Conductivity (W·m^{-1}·K^{-1})	N/A	$0.5 \cdot 2^n$ $n = 0, 1, \ldots 11$
Number of Fins	N/A	3, 4, 5, 6, 8, 10, 12
Fin Length (mm)	N/A	$1.735 + 0.0198 \cdot n$ $n = 0, 1, \ldots 100$
Fin Thickness (µm)	N/A	$59.4 + 1.98 \cdot n$ $n = 0, 1, \ldots 270$

The BISON simulations conducted in this work were based on a generic input file developed for predicting thermal performance of the UO$_2$ with conductive inserts. This generic input file was constructed such that only the mesh and thermal conductivity of

the conductive inserts needed to be modified between cases, which was achieved by implementing a Python script to modify input files and the fuel mesh. Cubit was used to change the geometry and mesh of the UO_2 fuel, cladding, and conductive inserts [20]. Each geometry consisted of a single UO_2 pellet in length, with other geometric dimensions in Table 2. Due to the size and number of conductive fins used in the simulations, different meshing techniques had to be used in Cubit to avoid a negative Jacobian or inverted element. This condition and the need for better consistency led to using the Tetmesh scheme within Cubit with a mesh size of four, which was applicable for all 2.56 million BISON simulations. This combination led to zero negative Jacobian errors. The boundaries and sidesets used in the BISON simulations had to be manually set in Cubit due to surfaces being renumbered after symmetry cuts were performed. The surfaces used for the coolant channel boundary condition and gap heat transfer between the fuel and the cladding were specified in Cubit so that boundaries called within BISON could be mapped to the geometry [20].

The BISON simulations were conducted to model the thermal characteristics of the fuel, and only the thermal solution is considered in this work. Thermomechanical modeling is planned for a later date to include thermal expansion, fuel swelling, delamination, FGR, and other thermomechanical models. The coolant condition of the generic input file utilized a convective heat flux boundary condition with a constant temperature of 640 K on the outer cladding wall [21]. This simulated a constant temperature imparted by a coolant channel. Heat transfer was allowed to occur radially from the outer fuel radius to the inner cladding wall using GapHeatTransferLWR, which allows for a layer of helium between the UO_2 pellet and the inner cladding wall [19,21]. Pellet–pellet interaction was not included in this study, as the thermal feedback between pellets is not significant to radial heat transfer. The thermal conductivity of helium is temperature dependent and is considered in the heat transfer calculations. The heat generated within the UO_2 fuel pellet was modeled with a volumetric heat source, which couples the fission rate (2.33716×10^{19} m^{-3}) and energy per fission (3.2×10^{-11} J) to produce heat within the fuel. The LHGR is then multiplied by the fission rate to generate the pin power. To keep the LHGR constant throughout all the BISON simulations despite the changing volume of the UO_2 pellets, the aforementioned base fission rate had to be scaled appropriately to accommodate the conductive inserts. The LHGR was ramped up from 0 to 50 kW·m^{-1} in 10,000 s to assist with BISON convergence, then allowed to operate for another 1000 s in order to reach the steady-state solution. The conductive inserts in the UO_2 pellet were assumed to afford perfect heat transfer (between the UO_2 and the insert) based on a complete absence of cracking or delamination. The same assumption was used previously, and a discussion on its validity is provided below [11].

Delamination was modeled by increasing the gap size between the conductive fins and the UO_2 fuel matrix to assess the effect delamination has on peak fuel temperature, with the delamination gap varying between 0 and 100 μm. An example geometry is seen in Figure 2. Conductive heat transfer through the delamination gap was modeled as a solid matrix with the material properties of helium, including a temperature dependent thermal conductivity. A solid matrix was chosen to model conductive heat transfer through the delamination gap due to simplicity. The alternative would require adding an additional conduction heat transfer (GapHeatTransferLWR) action to allow for heat transfer to occur between the conductive fin surfaces and the UO_2 fuel, with helium acting as a gap. This will be implemented in future work, as the difference in thermal expansion of the conductive fins and UO_2 fuel and FGR causes an uneven delamination gap, which is accounted for within the BISON GapHeatTransferLWR action.
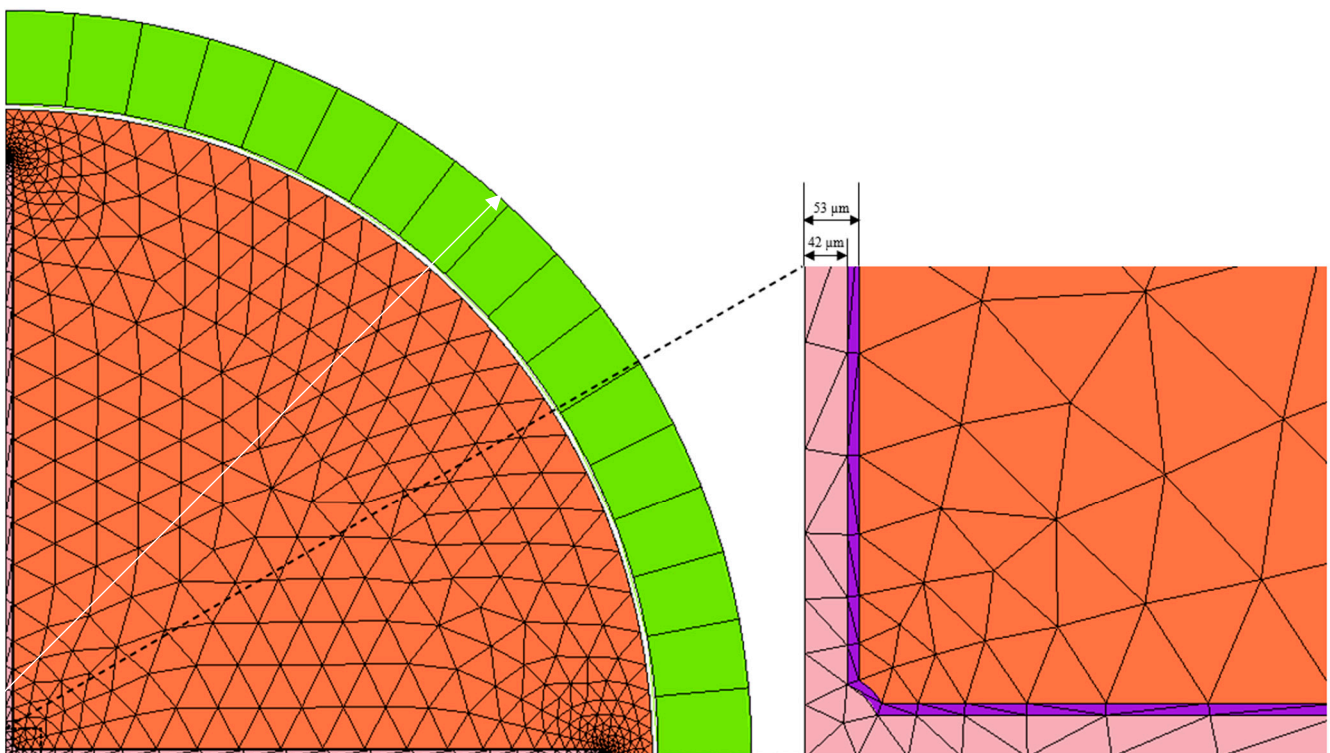
Figure 2. BISON mesh four fins with radial temperature sampling (**left**) and 11 μm delamination of fins (**right**).

The BISON code allows each material within the fuel element to be specified with respect to its thermal properties. The UO_2 pellet, conductive insert, and cladding wall were defined on separate blocks within Cubit, and each was given its own material within BISON. The UO_2 pellet used the FINK_LUCUTA thermal conductivity model in BISON, which is temperature, burnup, and porosity dependent, with an initial porosity of 0.05 [22]. For the conductive insert and the cladding, the thermal conductivity of each material was individually set, with the conductive insert's thermal conductivity being dependent on the conductive insert material, and the thermal conductivity of the cladding fixed at 16 W·m^{-1}·K^{-1}.
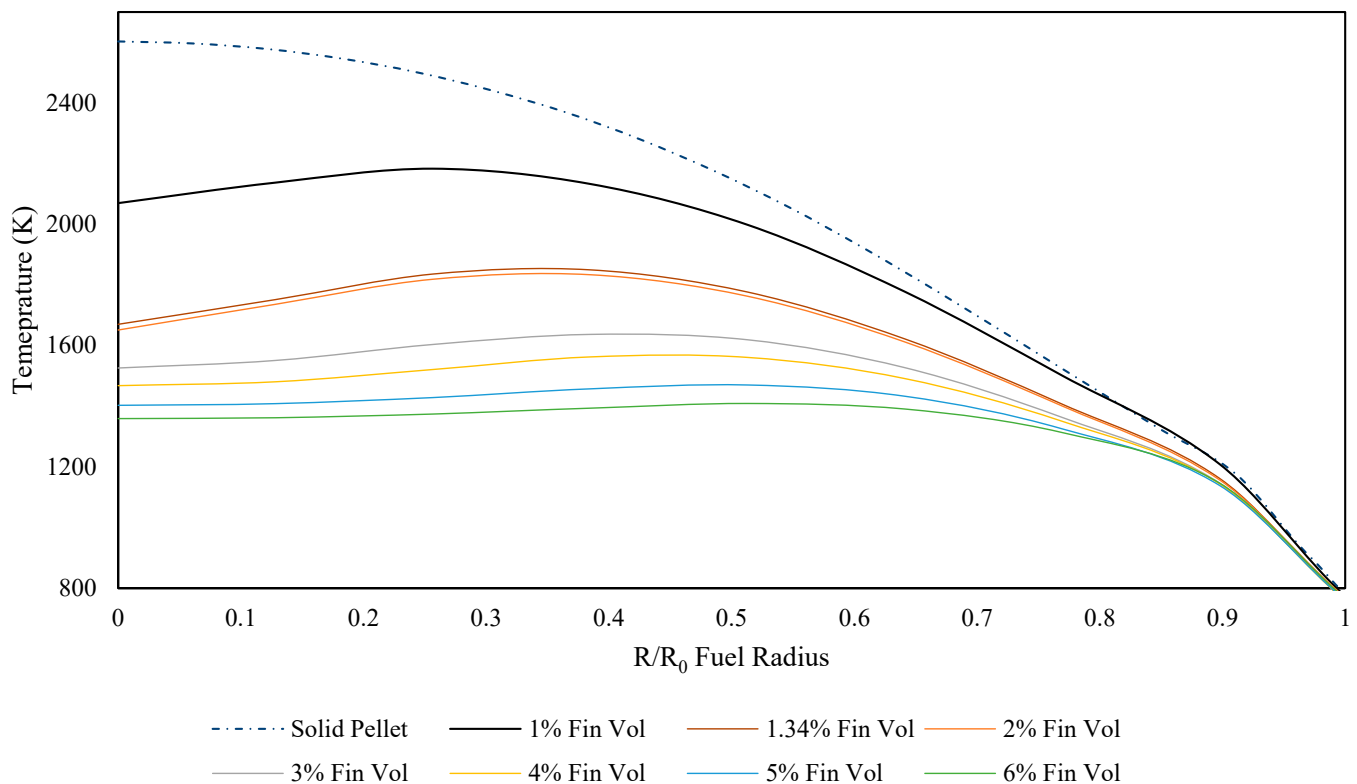
The radial temperature profile of the UO_2 fuel pin is reported along the path bisecting any two adjacent conductive inserts, as shown in Figure 2 for the case with four conductive inserts. As may be expected, this path locates the maximum temperature radial profile. Each radial temperature profile was generated using a VectorPostProcessor specified within the BISON input file and output as a CSV once the simulation completed. The maximum temperature from the radial temperature profile was recorded, and the temperature gradient was computed using interpolate spline from Python's SciPy library by taking the derivative of the radial temperature profile in respect to the fuel radius.

3. Results and Discussion

By utilizing the 2.56 million BISON simulations run with varying thermal conductivities, numbers, lengths, and thicknesses of the conductive fins, multiple questions can be answered in regard to how the choice of design can lower the peak UO_2 fuel temperature and average radial temperature gradient. The results presented in this manuscript discuss and show the optimal geometry for maximizing temperature reduction per conductive fin volume, as well as the optimal geometry for temperature reduction over a given conductive fin volume. Obviously, materials with higher thermal conductivities transfer heat more efficiently, and the simulations featuring conductive fins whose thermal conductivity was

equal to diamond had the lowest peak fuel temperature. The same intuition does not apply to achieving the lowest radial T gradient.

All 2.56 million results were post-processed using Python, and it was determined that three fins with a thermal conductivity of 1024 $W \cdot m^{-1} \cdot K^{-1}$, a length of 3.7125 mm, and a thickness of 59.4 μm gave the largest temperature reduction per insert volume percentage, being $-573.58 \frac{K}{\%_{finvol}}$ for a fin volume of 1.34%. The radial temperature profile for this combination is displayed in Figure 3. Although the peak fuel temperature from this case is not the lowest, it preserves the highest amount of fuel volume for the temperature reduction. It can be theorized and inferred from the results that this result may be improved by maximizing the surface-area-to-volume ratio of the fins, as is the case with any application to reduce local temperature. However, the lower bound on the fin thickness was set to ~60 μm due to the accuracy and resolution of current manufacturing techniques. Although the simulation results displayed in Figure 3 do not illustrate the lowest temperature achievable, the temperature reduction, as compared with a solid UO_2 pellet, is still 769.7 K for a fin volume of 1.34%. Within Figure 3, it can be seen that fin volumes of 1%, 1.34%, 2%, and 3% have a non-zero temperature gradient at the center of the fuel pellet. This non-zero temperature gradient is due to there being non-diametral symmetry due to utilizing three conductive inserts. Other geometry configurations within Figure 3 contained diametral symmetry by using an even number of fins.

Figure 3. Radial temperature profiles for optimal fixed pellet volumes.

The lowest peak fuel temperature and lowest radial temperature gradient for the UO_2 pellet were found to depend on the percent of the pellet volume replaced. At the lower fixed pellet volumes, only one unique solution emerged. At higher fixed pellet volumes, multiple solutions with different geometries provided comparable temperature results, but only the configurations with the lowest temperatures are displayed. For instance, a slightly shorter fin length and larger fin thickness yields an 8 K difference, which is shown in Table 3 for 3% fin volume. Geometric combinations of fixed UO_2 pellet volumes with the lowest peak fuel temperatures and the lowest radial temperature gradients are shown in

Table 3. It is important to note that the geometric configurations shown in Table 3 provided the lowest peak fuel temperature and radial temperature gradient for each material thermal conductivity, making the material thermal conductivity independent from the conductive insert geometry. This shows that the material properties of the conductive inserts are independent of the geometry for a radial heat transfer problem, as long as the conductive inserts have a greater thermal conductivity than the fuel.

Table 3. Fixed fin volume configurations with the lowest peak fuel temperatures and average radial temperature gradients.

Fin Volume (%)	Insert Thermal Con. ($W \cdot m^{-1} \cdot K^{-1}$)	Number of Fins	Fin Length (mm)	Fin Thickness (μm)	Peak Fuel Temperature (K)	Average Radial Temperature Gradient ($K \cdot m^{-1}$)
1	1024	3	2.82	59.4	2.18×10^3	-3.44×10^5
1.34	1024	3	3.71	59.4	1.84×10^3	-2.16×10^5
2	1024	3	3.71	91.1	1.83×10^3	-2.14×10^5
3	1024	3	3.69	83.1	1.65×10^3	-1.85×10^5
3	1024	5	3.71	81.2	1.64×10^3	-1.84×10^5
4	1024	6	3.71	89.1	1.56×10^3	-1.75×10^5
5	1024	8	3.71	83.2	1.47×10^3	-1.54×10^5
6	1024	10	3.71	79.2	1.41×10^3	-1.46×10^5

Conductive inserts with a lower thermal conductivity than the fuel would act as an insulator, and potentially increase fuel temperature depending on the chosen geometry. If the thermal conductivity was lowered, the same conductive fin configuration would still produce the greatest reduction in peak fuel temperature for that fin volume percentage. This is important when considering fabrication capability of the conductive inserts used within the fuel matrix. As the conductive fins increased in volume, geometries that led to the largest reductions in peak fuel temperature included having the longest fin length permittable. As the volume of the conductive fins increased, the number of fins used was also important in reducing the peak fuel temperature. In all the BISON simulations, the lowest peak fuel temperature calculated was 1200.3 K, with the major drawback of replacing 53.7% of the UO_2 pellet volume. Due to reactivity and burnup design criteria from other reports, no design configuration that replaced more that 6% of the pellet volume was considered [5].

Implementing the conductive fin inserts in the UO_2 pellet lowered the range of the radial temperature gradients. Adding conductive fins lowered the peak temperature of the UO_2 fuel, enabling the average radial temperature gradient to be reduced as well. The designs that led to the lowest peak fuel temperatures also resulted in the lowest average radial thermal gradients, thanks to each conductive fin being symmetrical and uniform in design. If the thickness of each conductive fin were a function of length, a different design would have resulted in lower average radial temperature gradients. The radial temperatures for fixed pellet volumes are shown in Figure 3 and temperature contour plots in Figure 4.

As the volume of the conductive fins increases, the peak fuel temperature moves radially towards the cladding. This is due to the conductive fins transferring heat away from the center of the fuel matrix to the outer edge. This is seen in the Figure 4 temperature contour plots for the different fin configurations in Table 3. Increasing the number of conductive fins decreased the radial temperature gradient within the fuel due to the addition of more heat spreaders. Utilizing a fin volume that is 1% of the fuel volume leads to a 420 K reduction in peak fuel temperature from a standard UO_2 pellet.
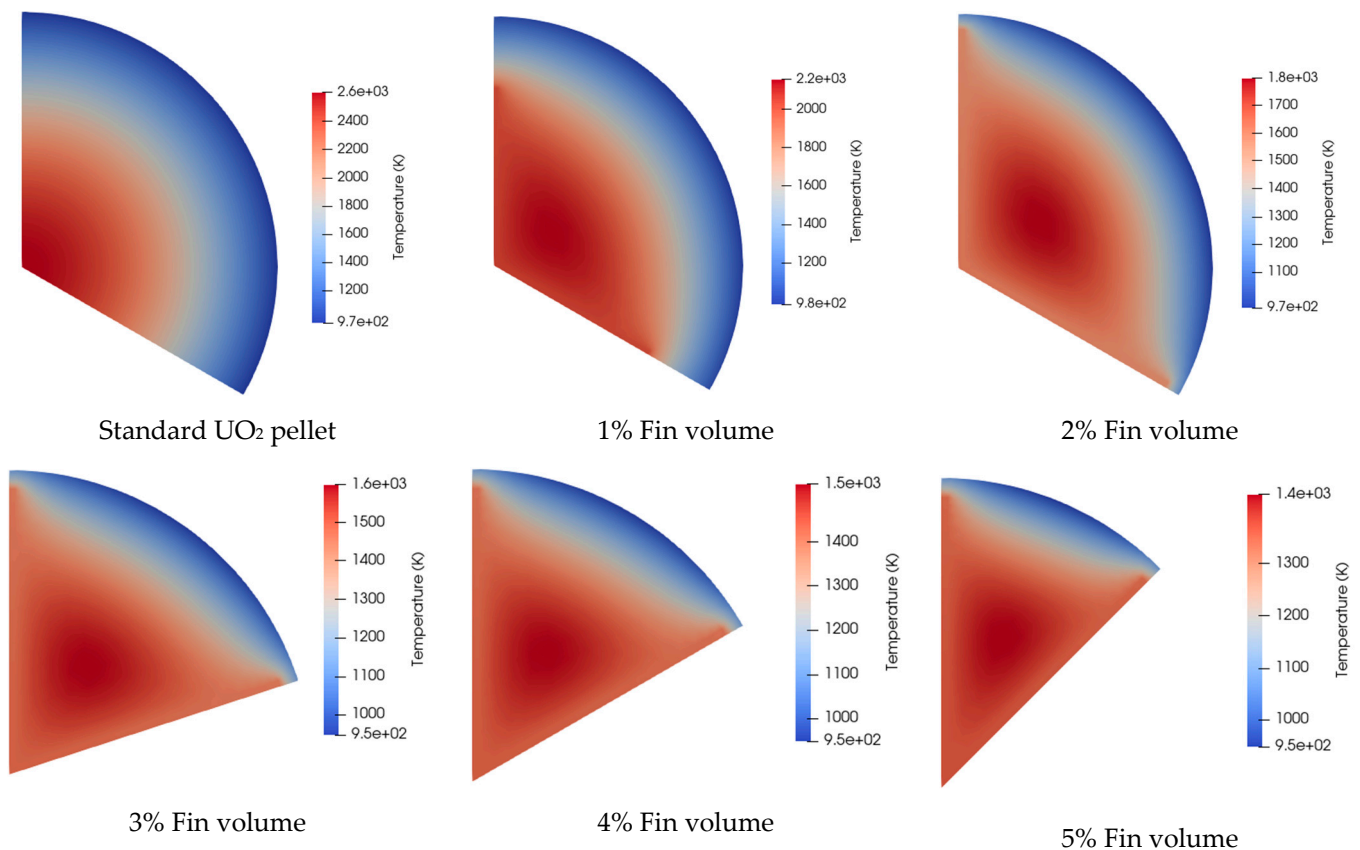
Figure 4. Fuel temperature contour plots with different conductive fin configurations from Table 3.

When comparing the conductive fin designs, the length of the fins was found to have the most significant impact on reducing the peak fuel temperature and average radial temperature gradient. This is due to the conductive fins transporting heat closer to the edge of the UO_2 pellet, creating less thermal resistance. Fin thickness and the number of fins also contributed to reducing peak fuel temperature. The desired amount of pellet volume being displaced determines the number and thickness of the fins. Using more fins leads to diminishing returns in reducing the peak fuel temperature, as the volume of the conductive fins increases in correlation with the increased fin thickness. In all cases, lower peak temperatures were achieved using the maximum thermal conductivity and length allowable in the BISON simulations.

The peak fuel temperature observed in the UO_2 pellet depended on the thermal conductivity, number, length, and thickness of the fins. To illustrate this, a polynomial regression describing the peak fuel temperature with the thermal conductivity of diamond was statistically modeled in Python using curve fit from scipy.optimize to represent the other peak fuel temperature results not presented in this work. Since using this Python library required assuming a polynomial to optimize the coefficients, the following non-linear third-order polynomial in Equation (1) was assumed in order to describe the peak fuel temperature. Due to the variables (number of fins, fin length, and fin thickness) having a non-linear dependent relationship with each other, nine additional terms were used in the polynomial regression (D-L and P-R). The constant in Equation (1) represents the peak fuel temperature of the UO_2 fuel without any conductive insert. A third-order polynomial was assumed due to the temperature having a second-order polynomial fit with respect to each independent variable. These fits are seen in Figures 5–7. In Equation (1), x is the number of fins, y is the fin length (m), and z is the fin thickness (m). The estimated coefficients for Equation (1) are listed in Table 4. The coefficients were optimized using 179,950 datapoints from all the simulations with the thermal conductivity of diamond. Equation (1) had a nonlinear regression coefficient of 0.9995. Equation (1) can be used to estimate the peak

fuel temperatures of different configurations not covered in this parametric study that fall within the bounds of the equation. The bounds of Equation (1) include a positive number of fins between 3 and 12, positive fin length between 1.75 and 3.7125 mm, and positive fin thickness between 59.4 and 594 μm. Although others may use Equation (1) outside of the suggested bounds, the range of these parameters encompasses the simulation results, and use of Equation (1) outside the bounds will carry uncertainty.

$$
\begin{aligned}
T_{Peak}(x,y,z) = \quad & Ax^3 + By^3 + Cz^3 + Dx^2y + Ex^2z + Fy^2x + Gy^2z + Hz^2x + Lz^2y + Mx^2 + Ny^2 + Oz^2 \\
& + Pxy + Qxz + Ryz + Sx + Ty + Uz + Vxyz + 2603.45
\end{aligned}
\tag{1}
$$
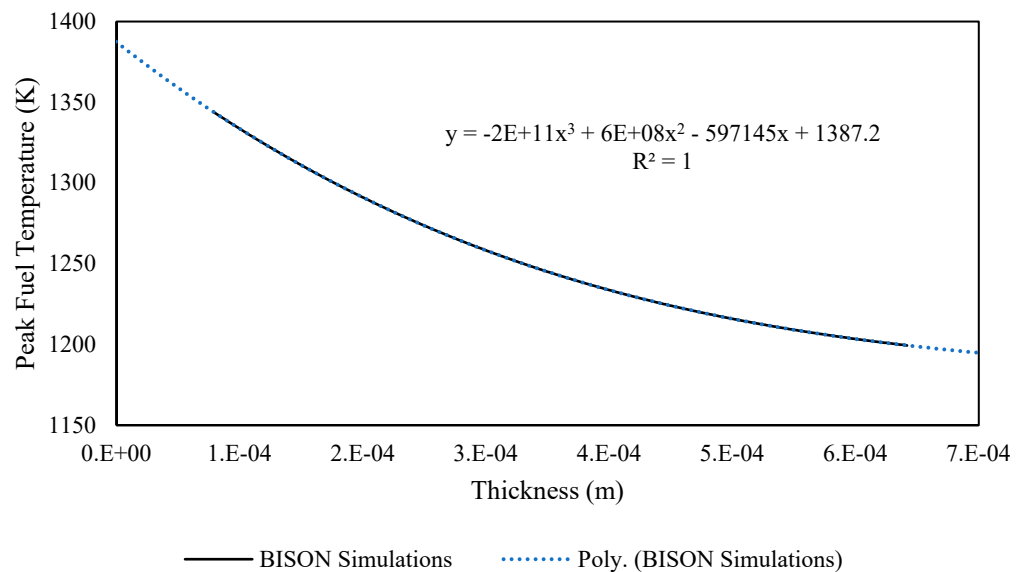
Figure 5. Peak fuel temperature with a fixed number of fins and a fixed fin length (12, 3.73 mm). Note the lessened temperature decrease with increasing thickness.
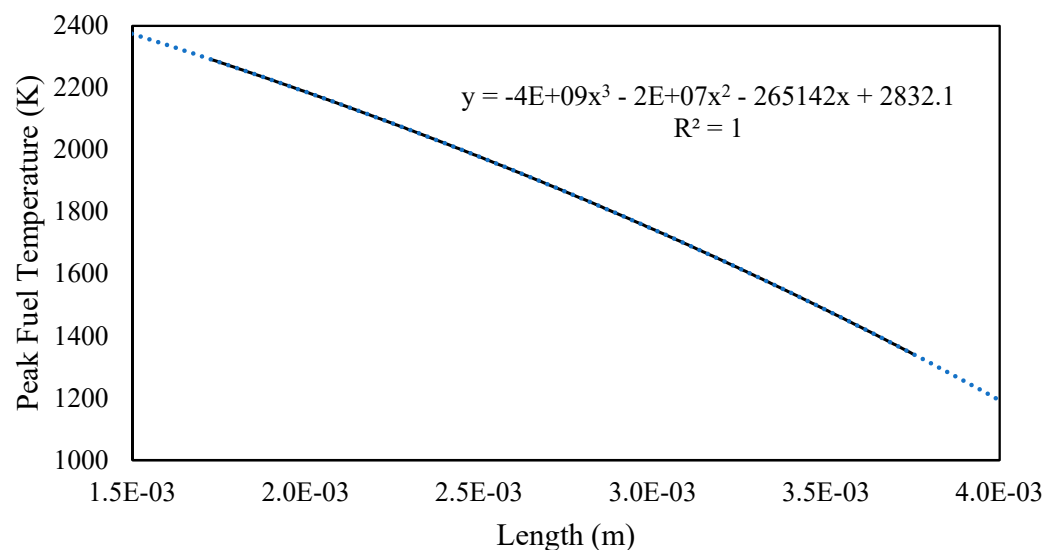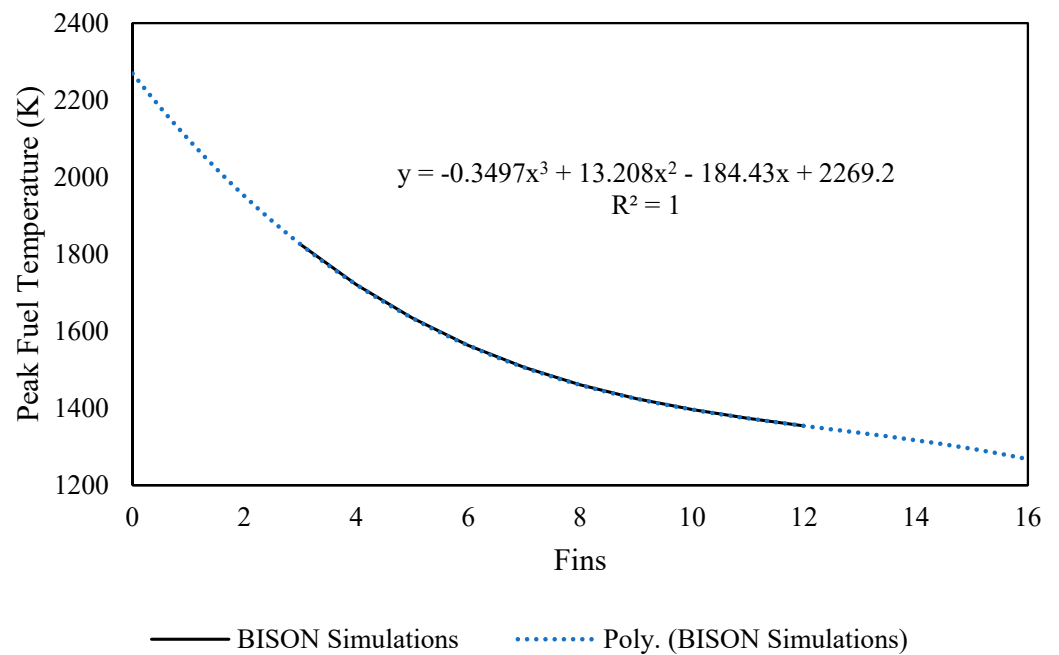

Figure 6. Peak fuel temperature with a fixed number of fins and a fixed fin thickness (12, 60 μm).

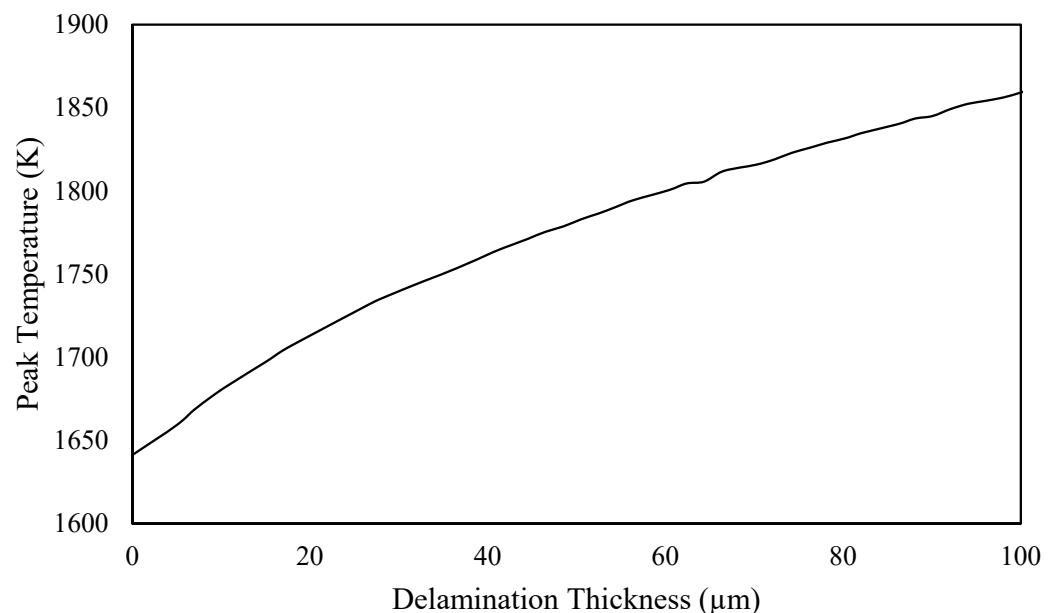**Figure 7.** Peak fuel temperature with a fixed fin length and fin thickness (3.73 mm, 60 μm).

Table 4. Coefficients for Equation (1), where "x" is the number of fins, "y" is fin length in meters, and "z" is fin thickness in meters. These coefficients were developed for the case of diamond.

Coefficient	Value	Standard Deviation
A	-3.50×10^{-1}	7.18×10^{-4}
B	5.59×10^{0}	1.84×10^{-2}
C	7.77×10^{0}	1.98×10^{-1}
D	2.02×10^{3}	3.07×10^{0}
E	1.39×10^{3}	1.23×10^{1}
F	-5.61×10^{4}	8.72×10^{1}
G	-1.25×10^{5}	2.75×10^{2}
H	-3.70×10^{9}	5.55×10^{7}
L	-3.97×10^{7}	3.60×10^{5}
M	1.16×10^{5}	6.43×10^{2}
N	1.37×10^{6}	1.41×10^{4}
O	3.02×10^{10}	2.94×10^{8}
P	-2.63×10^{8}	1.76×10^{6}
Q	-2.42×10^{11}	5.43×10^{9}
R	1.18×10^{8}	6.46×10^{6}
S	1.68×10^{5}	3.50×10^{3}
T	3.12×10^{7}	2.29×10^{5}
U	3.69×10^{10}	1.21×10^{9}
V	2.45×10^{7}	5.19×10^{4}

Each parameter used within the parametric study was varied with the other two parameters with fixed values to determine the impact each parameter had on peak fuel temperature. Equation (1) was compared with experimental data in Figures 5–7 and had

a linear regression of $R^2 = 1$. Equation (1) was also extended past experimental data bounds to show unphysical results using a polynomial fit, such as fins having a length and thickness with zero fins. However, Figures 5 and 7 show an apparent asymptotic limit to increasing the number of fins and fin thickness, suggesting diminishing returns. Any temperature benefits from increasing the number of fins beyond 6 or 8 and fin thickness beyond 600 μm would have to be weighed against the cost of fin and fuel fabrication. Figure 6 shows a steeper temperature decrease with increasing fin length. Long-term fuel and cladding performance would need to be investigated for cases in which the fins reached 90%, 95%, or 100% of the pellet diameter. It is conceivable that the fins could also touch the cladding, and all these cases would need to be assessed in terms of fabrication costs as well as fuel and cladding performance.

Delamination of the UO_2 fuel from the conductive insert was explored for the optimal 5% fin-volume case listed in Table 3, but with the thermal conductivity of molybdenum (128 $W \cdot m^{-1} \cdot K^{-1}$), and with helium filling the gap between the conductive fins and the UO_2 fuel. Helium gas was assumed between the conductive fins and the UO_2 matrix due to the fin length extending to the outer fuel radius. When thermomechanical modeling is performed later, fission gas composition produced inside the fuel matrix will be used to generate the thermal conductivity of the delamination gap. The addition of this would decrease the effectiveness of the conductive fins, due to xenon gas having a significantly lower thermal conductivity compared with helium. The helium delamination gap was modeled as a solid with a temperature-dependent thermal conductivity and only conductive heat transfer considered. Peak fuel temperature in relation to increasing delamination thickness (an increasing gap between the UO_2 and the insert) is shown in Figure 8 below. If a material with higher thermal conductivity was used for the conductive fins, delamination would cause a greater change in temperature due to the overall effective thermal conductivity of the conductive fins being reduced.

Figure 8. Peak fuel temperature with delamination for the optimal 5% fin geometry with molybdenum fins (128 $W \cdot m^{-1} \cdot K^{-1}$).

In addition to delamination being simulated with thermomechanical models in the future, thermal expansion, swelling, creep, FGR of the fuel, cladding, and conductive inserts were not included in this analysis. This was left for future work due to the amount of computational time required to simulate fully coupled thermomechanical simulations for all conductive insert combinations. However, the simplicity of only considering a steady state thermal solution within these results neglects phenomena caused by differences in

material properties and FGR of the fuel. Differences in material properties such as different thermal expansion coefficients and void swelling rates may lead to debonding of the UO_2 fuel and the conductive inserts, decreasing the effectiveness of the conductive insets. However, temperature is important for fission gas retention within the fuel, which can delay fission gas release longer if at a low enough temperature [10]. Once fission gas is released, the helium plenum becomes polluted, degrading the thermal conductivity of the gas gap. This leads to higher fuel temperatures during steady state operations and contributes to finer pellet fragmentation if a blowdown were to occur, hence the focus on temperature reduction within this work [10].

FGR from UO_2 fuel occurs above the Halden threshold, which is dependent on burnup [10]. At higher burnups at 60 MWd/kg UO_2, FGR does not occur until 1316 K [10]. This is significant as fission gas degrades the thermal conductivity of the gap between the fuel and the cladding and the delamination gap forming between the fuel and conductive inserts. However, if the fuel operated at 35 kW·m^{-1}, it is conceivable that the peak fuel temperature would be below this temperature threshold for standard operating conditions for certain conductive fin configurations.

This parametric study only consisted of uniform rectangular fins with varying geometries and thermal conductivities. Depending on customer needs such as lower temperature gradients, other conductive insert geometries should be explored, including fins with varying thicknesses and thermal conductivities over the length of the insert. Although implementing a more complex geometry or inserting a conductive insert with a higher thermal conductivity might decrease the peak fuel temperature and radial temperature gradient, the added material and manufacturing cost may deter potential customers from adopting them. A good example of this includes the process of manufacturing synthetic diamond and bonding it to UO_2 pellets through compression. Currently, INL facilities are set up for manufacturing molybdenum heat spreaders for a UO_2 and fabrication techniques would require substantial rework due to a material change. This has the result that using molybdenum inserts within a UO_2 matrix is more practical and marketable to potential customers. Depending on the application, a potential customer would have to conduct a performance-cost analysis for certain fabrication scenarios involving the inserts and UO_2 pellets.

When comparing results from these BISON simulations with previous results, the radial temperature profile presented in this work was found to be higher [11]. This is due to implementing a helium gap via the GapHeatTransferLWR, whereas previous work assumed that the UO_2 pellets had swollen and come into direct contact with the cladding material. The difference in results is expected as the helium gap acts as an insulator. A comparison is given in Figure 9.

The results presented in this work show that peak fuel temperature is reduced based on the geometry and the amount of fuel replaced by a more conductive material, with the geometry being bound by the same parameters within Equation (1). However, the concept of using conductive heat spreaders to reduce temperature in nuclear fuels can be applied to other fuel systems, or other problems that include a volumetric heat generation term. In addition, adding conductive inserts to a system that already has good heat transfer might not be worth the extra financial cost and development for a given temperature reduction. An example of this would be outfitting sodium bonded U-Pu-Zr fuel slugs with molybdenum fins, as the effective radial thermal conductivity of that system is above 20 W·m^{-1}·K^{-1}.

Since the current the BISON simulations evaluated only the thermal solutions, thermal-mechanical properties such as swelling, thermal expansion, creep, and FGR need to be coupled into the most optimal solution and run through a typical LWR power cycle. Other improvements to the BISON simulation would include the variable thermal conductivity of the insert as a function of temperature, a single-pass flow boundary condition on the outside of the cladding, irradiation physics, and stacks of multiple UO_2 pellets [23]. This much more comprehensive evaluation would be compared with a

thermal, steady-state solution, and that simulation would be constructed to correspond to irradiation experiments currently being conducted at INL within the Advanced Test Reactor and the Transient Reactor Test Facility.
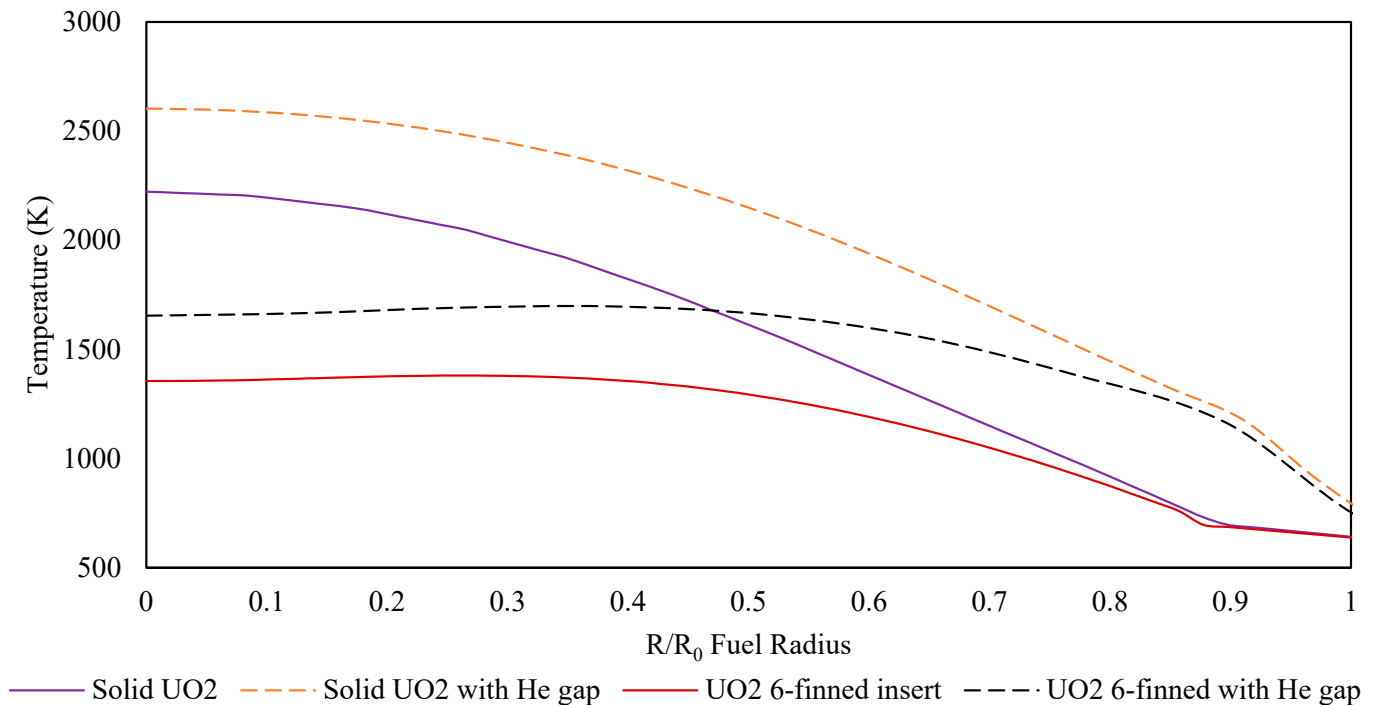
Figure 9. Implementation of a helium gap with a molybdenum insert, 3.75-mm fin length, and 114-μm fin thickness.

4. Conclusions

Using BISON, the parametric study of conductive inserts successfully identified the optimal geometry for minimizing the peak fuel temperature of a UO_2 pellet for fixed pellet volumes, using conductive inserts that occupy 1–6% of the UO_2 fuel volume. The thermal conductivity of the conductive insert used played a trivial role in reducing the peak fuel temperature and minimizing the radial temperature gradient, provided it was at least greater than the thermal conductivity of the fuel. It was found that the thermal conductivity of the conductive inserts and conductive insert geometry were independent of each other in reducing the peak fuel temperature and the radial temperature gradient. The length of the conductive inserts was found to be the most impactful parameter for reducing the peak fuel temperature. Depending on the amount of fuel volume being replaced by the conductive inserts, the number of conductive fins should be increased once increasing the thickness of the inserts begins to result in diminishing returns. This is determined by the geometry and dimensions of the UO_2 fuel pin. The best conductive insert configuration for 6% fuel volume reduced the peak fuel temperature by 1197 K when compared with the solid UO_2 pellet.

The temperatures presented in this work were found to be higher than in previous work, due to implementing a helium gap between the fuel and the cladding. Delamination was found to not significantly impact the peak fuel temperature of UO_2 for a LHGR of 50 kW·m^{-1}. The optimal geometry should later be coupled with mechanical models available in BISON for full fuel performance evaluation and then compared with other designs. This is crucial to understanding the long-term impact on fuel performance with fission gas release being delayed to higher burnups. Experimental validation with post irradiation examination data is also planned and will help model delamination within the fuel pin. The data generated from this parametric study are to serve as the base training data for a machine learning reinforcement optimization to generate more complex

geometries that will further reduce peak fuel temperatures. In any real application, the material/manufacturing costs of the conductive insert geometry will be an important consideration in cost-benefit fuel performance analyses for such designs.

Abbreviations

ATR	Advanced Test Reactor
FGR	Fission Gas Release
INL	Idaho National Laboratory
LWR	Light-Water Reactor
LHGR	Linear Heat Generation Rate

References

1.   Ishimoto, S.; Hirai, M.; Ito, K.; Korei, Y. Thermal Conductivity of UO_2-BeO Pellet. *J. Nucl. Sci. Technol.* **1996**, *33*, 134–140. [CrossRef]
2.   Kim, D.-J.; Rhee, Y.W.; Kim, J.H.; Kim, K.S.; Oh, J.S.; Yang, J.H.; Koo, Y.-H.; Song, K.-W. Fabrication of micro-cell UO_2–Mo pellet with enhanced thermal conductivity. *J. Nucl. Mater.* **2015**, *462*, 289–295. [CrossRef]
3.   Yeo, S.; Baney, R.; Subhash, G.; Tulenko, J. The influence of SiC particle size and volume fraction on the thermal conductivity of spark plasma sintered UO_2–SiC composites. *J. Nucl. Mater.* **2013**, *442*, 245–252. [CrossRef]
4.   Cartas, A.; Wang, H.; Subhash, G.; Baney, R.; Tulenko, J. Influence of Carbon Nanotube Dispersion in UO_2–Carbon Nanotube Ceramic Matrix Composites Utilizing Spark Plasma Sintering. *Nucl. Technol.* **2015**, *189*, 258–267. [CrossRef]
5.   Morrell, M.E. *Phase 1A Final Report for the AREVA Team Enhanced Accident Tolerant Fuels Concepts*; AREVA Federal Services LLC.: Charlotte, NC, USA, 2015.
6.   Yang, J.H.; Kim, D.-J.; Kim, K.S.; Koo, Y.-H. UO_2–UN composites with enhanced uranium density and thermal conductivity. *J. Nucl. Mater.* **2015**, *465*, 509–515. [CrossRef]
7.   Iwasaki, K.; Matsui, T.; Yanai, K.; Yuda, R.; Arita, Y.; Nagasaki, T.; Yokoyama, N.; Tokura, I.; Une, K.; Harada, K. Effect of Gd_2O_3Dispersion on the Thermal Conductivity of UO_2. *J. Nucl. Sci. Technol.* **2009**, *46*, 673–676. [CrossRef]
8.   George, N.M.; Terrani, K.; Powers, J.; Worrall, A.; Maldonado, I. Neutronic analysis of candidate accident-tolerant cladding concepts in pressurized water reactors. *Ann. Nucl. Energy* **2015**, *75*, 703–712. [CrossRef]
9.   Alrwashdeh, M.; Alameri, S.A. SiC and FeCrAl as Potential Cladding Materials for APR-1400 Neutronic Analysis. *Energies* **2022**, *15*, 3772. [CrossRef]
10.   Rest, J.; Cooper, M.; Spino, J.; Turnbull, J.; Van Uffelen, P.; Walker, C. Fission gas release from UO_2 nuclear fuel: A review. *J. Nucl. Mater.* **2018**, *513*, 310–345. [CrossRef]
11.   Medvedev, P.G.; Mariani, R.D. Conductive inserts to reduce nuclear fuel temperature. *J. Nucl. Mater.* **2020**, *531*. [CrossRef]
12.   Malerba, L.; Al Mazouzi, A.; Bertolus, M.; Cologna, M.; Efsing, P.; Jianu, A.; Kinnunen, P.; Nilsson, K.-F.; Rabung, M.; Tarantino, M. Materials for Sustainable Nuclear Energy: A European Strategic Research and Innovation Agenda for All Reactor Generations. *Energies* **2022**, *15*, 1845. [CrossRef]
13.   Mariani, R.D.; Medvedev, P.G.; Porter, D.L.; Hayes, S.L.; Cole, J.I. *Nocel Accident-Tolerant Fuel Meat and Cladding*; Idaho National Lab. (INL): Idaho Falls, ID, USA, 2013.
14.   Mariani, R.D. Accident-tolerant Oxide Fuel and Cladding. US 9666310B1, 30 May 2017.
15.   Nuclear Energy Agency. *State-of-the-Art Report on Light Water Reactor Accident-Tolerant Fuels*; Nuclear Energy Agency: Paris, France, 2018.
16.   Leibowitz, L.; Blomquist, R.A. Thermal conductivity and thermal expansion of stainless steels D9 and HT9. *Int. J. Thermophys.* **1988**, *9*, 873–883. [CrossRef]

17. Hofman, G.L.; Billone, M.C.; Koenig, J.F.; Kramer, J.M. *Metallic Fuels Handbook*; Argonne National Lab. (ANL): Argonne, IL, USA, 2019.

18. Che, J.; Cagin, T.; Deng, W.Q.; Goddard, W.A.; William, A. Thermal Conductivity of Diamond and Related Materials from Molecular Dynamics Simulations. *J. Chem. Phys.* **2000**, *113*, 6888–6900. [CrossRef]

19. Hales, J.; Novascone, S.; Spencer, B.; Williamson, R.; Pastore, G.; Perez, D. Verification of the BISON fuel performance code. *Ann. Nucl. Energy* **2014**, *71*, 81–90. [CrossRef]

20. Sandia National Laboratory. *CUBIT TM 15. 7 User Documentation*; Sandia National Laboratory: Albuquerque, NM, USA, 2021.

21. Hales, J.D.; Gamble, K.A.; Spencer, B.W.; Novascone, S.R.; Pastore, G.; Liu, W.; Gardner, R.J. *BISON Users Manual—BISON Release 1.2*; Idaho National Laboratory: Idaho Falls, ID, USA, 2015.

22. Fink, J. Thermophysical properties of uranium dioxide. *J. Nucl. Mater.* **2000**, *279*, 1–18. [CrossRef]

23. Hales, J.; Tonks, M.; Gleicher, F.; Spencer, B.; Novascone, S.; Williamson, R.; Pastore, G.; Perez, D. Advanced multiphysics coupling for LWR fuel performance analysis. *Ann. Nucl. Energy* **2014**, *84*, 98–110. [CrossRef]